Journal of Computer and Communications, 2022, 10, 162-171
https://www.scirp.org/journal/jcc
ISSN Online: 2327-5227
ISSN Print: 2327-5219

The Impact of Turbulence on MANET FSO Networks Using NS-3

Lamiae Bouanane[1], Fouad Mohamed Abbou[2], Farid Abdi[1], Kevin Smith[2], Abdelouahab Abid[3]

[1]Faculty of Sciences and Technologies, Sidi Mohamed Ben Abdellah University, Fes, Morocco
[2]School of Science and Engineering, Al Akhawayn University, Ifrane, Morocco
[3]Information Technology, Islamic University of Medina Saudi Arabia, Medina, Kingdom of Saudi Arabia
Email: lamiae.bouanane@gmail.com

How to cite this paper: Bouanane, L., Abbou, F.M., Abdi, F., Smith, K. and Abid, A. (2022) The Impact of Turbulence on MANET FSO Networks Using NS-3. *Journal of Computer and Communications*, **10**, 162-171.
https://doi.org/10.4236/jcc.2022.1010011

Received: September 6, 2022
Accepted: October 28, 2022
Published: October 31, 2022

Abstract

In this paper, the impact of atmospheric turbulence is investigated and analyzed for the Free Space Optical Mobile Ad Hoc Networks (FSO MANET) using the Network Simulator NS-3. The FSO channel random intensity fluctuations have been modeled using the Exponentiated Weibull (EW) distribution. Further, the FSO module has been implemented and integrated with NS3 using the FSO propagation model and the FSO error models. The computation of the key performance indicators (KPI) mainly the throughput and the packet delivery ratio (PDR) shows that the network density affects the network performance. Its effect was illustrated for the different turbulence regimes, strong and weak. It is found that the throughput and PDR values decrease as the number of mobile nodes becomes larger. For instance, at 150 kbps and in the presence of strong turbulence with 25, 50, and 75 nodes, the PDRs are 77%, 76%, and 73% respectively. Moreover, the throughput and PDR values in the strong turbulence regime are lower than those in the weak turbulence regime for the same date rate. The throughput in the strong turbulence regime with 75 mobile nodes at the data rate 150 kbps is 2100 kbps while it is 2300 kbps in the weak turbulence mode at the same rate.

Keywords

MANET, FSO, Turbulence, Exponentiated Weibull, BER, Packet Delivery Ratio, NS-3

1. Introduction

The fifth generation (5G) mobile networks have emerged as a viable option to satisfy the Quality of Service (QoS) requirements for different classes of services of data traffic. The 5G technology offers various promising services such as massive system capacity, huge device connectivity, high-level security, ultra-low latency, and extremely low power consumption [1]. To achieve this, 5G communication networks require high capacity cellular backhauls to ensure reliability for the massive number of devices into the core network [2]. FSO communication technology has emerged as a promising cost-effective solution to mitigate conventional Radio Frequency (RF) spectrum scarcity. FSO is a line of sight (LOS) point-to-point transmission system that provides outstanding communication features such as ultra-high data rate, low latency, low cost, and lower power consumption while offering reliable security, electromagnetic interference free transmission, and high system efficiency thanks to its broad optical spectrum [3]. The major FSO limitations are due to the atmospheric turbulence, the atmospheric attenuation resulting from the diverse weather conditions and the physical obstructions. These environmental factors highly degrade the FSO link performance and may result in link unavailability.

MANETs are multihop networks that are built "on the fly" and they do not have any backbone infrastructure or central coordinator. Research in MANET and FSO is of great importance for bandwidth intensive applications like multimedia. Free Space Optical Mobile Ad Hoc network (FSO MANET) was originally designed for military applications and Delay Tolerant Networks. Today, they can also be used in emergency disaster relief efforts. An example of an FSO MANET application could be a network made up of mobile FSO nodes such as robots. This can serve as a viable communication system for medical experiments.

The research work [4] demonstrates that FSO in multihop communication achieves a significant reduction in the mean bit error rate (BER) and reduces the variance of the bit error rate. In this paper [5], the authors proposed new FSO node design that uses spherical surfaces covered with transmitter and receiver modules for maintaining optical links even when nodes are moving in an FSO MANET communication system. A similar work [6] was proposed later that studies a multi-transceiver spherical FSO structure as a building block for enabling optical spectrum in mobile ad-hoc networking. FSO MANETs are implemented using extensions for free space optical structures along with NS-2.34 provided in the package for FSO extensions. The free space optical node uses multiple interfaces for transmission and reception of packets. The authors in [7] aimed at designing an efficient routing in FSO MANET. This paper proposes a method to find the stable path as well as stable nodes between the source and destination. Another research work [8] developed and simulated a geographical routing protocol called Dir-DREAM (Directional Distance Routing Effect Algorithm for Mobility) for the FSO MANETs where nodes have multiple FSO Antennas. The proposed protocol uses node's location information and past information of interfaces over which packets from nodes are received for routing. Most of these papers on FSO MANETs discuss the directionality and LOS but few papers tackled the effect of the atmospheric turbulence on the performance of FSO MANETs.

The atmospheric turbulence occurs due to inhomogeneities of pressure and temperature. Its effect induces random variations of the air's refractive index, that cause fluctuations in the amplitude and phase of the optical signal at the receiver end, known as atmospheric scintillation [9].

Scintillation fluctuations can be categorized into three regimes: weak, moderate, and strong. This paper presents the FSO channel that models the random intensity fluctuations using the Exponentiated Weibull (EW) distribution. It has been shown that the EW is a good distribution to model the FSO signal irradiance under the three turbulence regimes while using the aperture averaging technique [10]. Aperture averaging is one of the most used measures to mitigate the scintillation effects on the optical beam [11]. It consists of increasing the area of the detection plane to collect the signal as much as possible.

For the simulation of the FSO MANETs, the Network Simulator 3 was selected as it provides models that cope with real world philosophy and concepts. NS-3 does not have an FSO module. Therefore, the FSO module in NS-3 was first implemented.

Further, the remainder of this paper is structured as follows. Section 2 presents the theoretical analysis that details the computation of the average BER. Section 3 presents the FSO MANET network architecture while Section 4 analyses the performance of the proposed work through simulations. Section 5 presents the conclusion followed by references.

2. FSO Channel Model

The received signal power Pr of an FSO link can be computed as follows [12]:

$$P_r = P_t\left(\frac{D}{L\theta}\right)^2 \tau_t \tau_r 10^{-\gamma(\lambda)\cdot\frac{L}{10}} \tag{1}$$

where P_t is the transmitter single power, θ is the beam divergence angle, τ_t and τ_t are the antennas gains of transmitter and receiver, respectively, $\gamma(\lambda)$ is the transmitted light's attenuation and L is the link distance.

To quantify the effect of intensity fluctuations, the scintillation index is usually used [13]. Another important parameter is the Rytov variance, σ_R^2. In the weak turbulence regime, the scintillation index is proportional to the Rytov variance. Rytov is calculated as [14]:

$$\sigma_1^2 = 1.23 C_n^2 k^{\frac{7}{6}} L^{\frac{11}{6}} \tag{2}$$

where C_n^2 is the turbulence strength, $k = 2\pi/\lambda$ is the optical wave number, and L is the distance between the transmitter and the receiver.

The probability density function (PDF) of the received irradiance I using the EW is expressed as [15]:

$$f(I) = \frac{\alpha\beta}{\eta}\left(\frac{I}{\eta}\right)^{\beta-1} \exp\left[-\left(\frac{I}{\eta}\right)^{\beta}\right] \times \left\{1-\exp\left[-\left(\frac{I}{\eta}\right)^{\beta}\right]\right\}^{\alpha-1} \tag{3}$$

where α and β are shape parameters, and η is the scale parameter.

The shape parameter α is defined as [16]:

$$\alpha = \frac{7.220\sigma_I^{\frac{2}{3}}}{\Gamma\left(2.487\sigma_I^{\frac{2}{6}} - 0.104\right)} \tag{4}$$

The shape parameter β is given by:

$$\beta = 1.012\left(\alpha\sigma_I^2\right)^{\frac{-13}{25}} + 0.142 \tag{5}$$

where σ_I^2 is the scintillation index.

The scale parameter η is calculated as:

$$\eta = \frac{1}{\alpha\Gamma\left(1+\frac{1}{\beta}\right)g(\alpha,\beta)} \tag{6}$$

where $g(\alpha,\beta)$ is defined by:

$$g(\alpha,\beta) = \sum_{i=0}^{\infty} \frac{(-1)^i (i+1)^{\frac{1+\beta}{\beta}\Gamma(\alpha)}}{i!\Gamma(\alpha-i)} \tag{7}$$

The BER of FSO systems with IM-DD and OOK modulation in the presence of Additive White Gaussian Noise (AWGN) can be calculated as [17]:

$$P_e = \frac{1}{2}\operatorname{erfc}\left(\frac{\sqrt{\mathrm{SNR}_0}}{2\sqrt{2}}\right) \tag{8}$$

where erfc is the complementary error function and SNR_0 is the signal-to-noise ratio in the absence of turbulence.

The SNR can be computed as:

$$\mathrm{SNR}_0 = \frac{R\left(P_r R_d\right)^2}{4KTB} \tag{9}$$

where B represents the bandwidth, T is the absolute system temperature, R is the load resistor, K is the Boltzmann's constant, R_d is responsivity of the detector and P_r is the received power.

Over the turbulent FSO links, the BER is considered a conditional probability needs to be averaged over the PDF of the signal, to get the unconditional BER. In the presence of turbulence, the BER is estimated as [18]:

$$\mathrm{BER} = \int_0^{\infty} f(I) P_e \mathrm{d}I \tag{10}$$

Doing the necessary mathematical transformation and approximation, the BER could be written as:

$$\mathrm{BER} = \frac{\sigma_n}{\sqrt{2\pi}R_d P_r}\sum_{k=1}^{n} W_k \left\{1-\exp\left[-\left(\frac{\sqrt{2}\sigma_n}{R_d P_r}\sqrt{z_k}\right)^{\beta}\right]\right\}^{\alpha} \tag{11}$$

where z_k is the k-th root of the generalized Laguerre polynomial $L_n^{-\frac{1}{2}}(z)$ and W_k is computed as [19]:

$$W_k = \frac{\Gamma\left(n+\frac{1}{2}\right)z_k}{n!(n+1)^2\left[L_{n+1}^{-\frac{1}{2}}(z_k)\right]^2} \tag{12}$$

3. Network Architecture

Considering the FSO channel model described in the previous section, the NS3 FSO error model is used to compute the packet error rate (PER) of the FSO links between FSO nodes. The PER is compared to a random variable to decide about the acceptance or the rejection of packets. In other words, strong turbulence induces higher PER and leads to high packet lost rates. Further, in order to simulate the FSO model in a MANET scenario in NS-3, the FSO nodes were randomly deployed in a 5000 by 5000 m^2 terrestrial area. Whereby the number of mobile nodes is set to 25, 50 and 75, the average transmission radius of each FSO node is set up to 4000 m. The mobility speed was set to 20 m/s. Ten different source/destination pairs were defined. Furthermore, the simulation is repeated 100 times to obtain statistically accurate and stable results. The simulation time is set to be 120 seconds. Strong and weak turbulence modes have been considered. The main KPIs considered are the throughput and PDR. In order to calculate the KPIs, the Network Performance Analysis Framework (NPAF) NS-3 module has been used [20]. **Figure 1** shows the 25 FSO mobile nodes random set up and **Table 1** presents some of the main parameter's values used in the simulation.

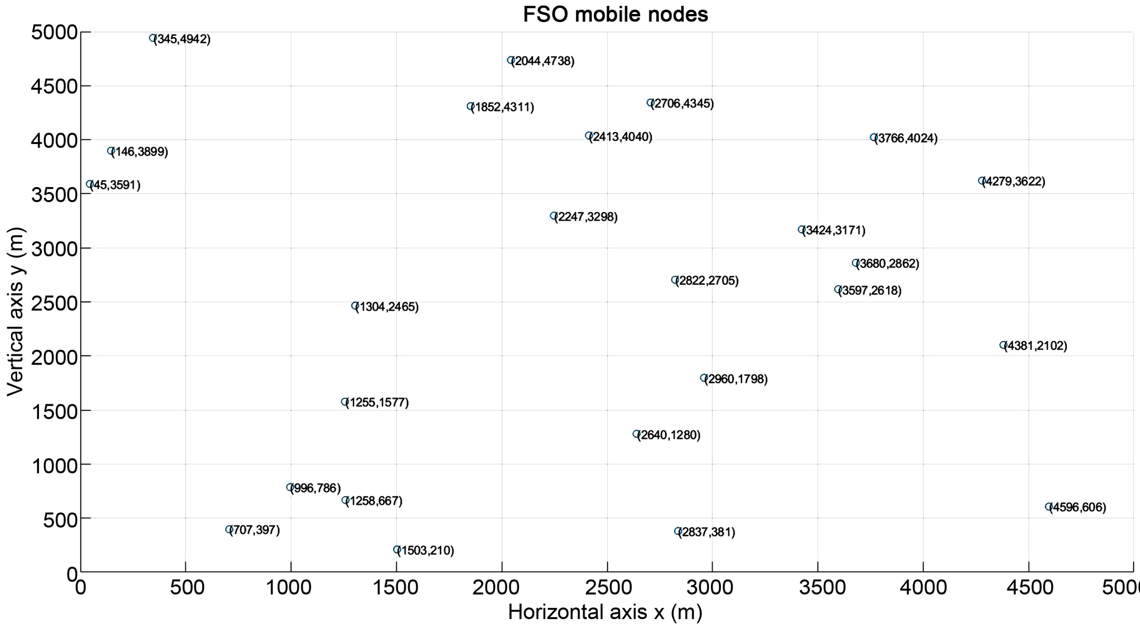

Figure 1. FSO mobile nodes in a random position set up (case of 25 nodes).

Table 1. Simulation parameters.

Parameter	Value
Transmitted power	10 dBm
Receiver diameter	20 cm
Attenuation model	Kim
Radius of transmission	4000 m
Traffic type	CBR
Packet size	1024
Simulation time	120 s

4. Results and Discussion

- Throughput and PDR versus data rate (strong turbulence)

According to Figure 2, the throughput increases as the data rate increases in the presence of the strong turbulence. However, this increase depends on the network density. Further, the throughput gets lower as the number of mobile nodes becomes larger. So, at 150 kbps and with a number of nodes of 75 nodes, the achieved throughput is 2100 kbps.

Further, as shown in Figure 3, the PDR is plotted versus data rate for different number of mobile nodes. It is clear that as the data rate increases, the PDR decreases. However, the best PDR is obtained when the number of mobile nodes is the smallest. For instance, at 150 kbps and in the presence of strong turbulence with 25, 50, and 75 nodes, the PDRs are 77%, 76%, and 73% respectively.

- Throughput and PDR versus data rate (weak turbulence)

As shown in Figure 4, the throughput increases as the data rate increases in the presence of the weak turbulence. However, this increase depends on the network density. Further, the throughput gets lower as the number of mobile nodes becomes larger. Further, as shown in Figure 5, the PDR is plotted versus data rate for different number of mobile nodes. It is clear that as the data rate increases, the PDR decreases. However, the best PDR is obtained when the number of mobile nodes is the smallest.

5. Conclusions

In this paper, the impact of atmospheric turbulence is investigated in the context of FSO MANETs in NS-3. The proposed FSO channel model uses the EW intensity distribution to model the atmospheric channel turbulence. The FSO nodes were randomly located and were moving in random directions. Further, the network density varied from 25, 50 to 75 nodes. Performance results show that the throughput and PDR values get lower as the number of mobile nodes becomes larger. It is also found that the throughput and PDR values in the strong turbulence regime are lower than those in the weak turbulence regime for

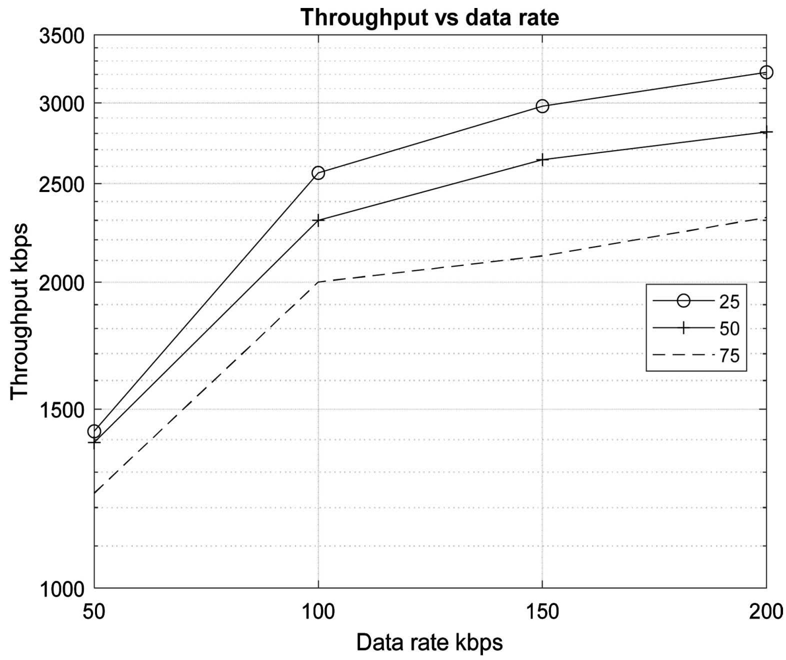

Figure 2. Throughput versus data rate for different network node density in the presence of strongturbulence.

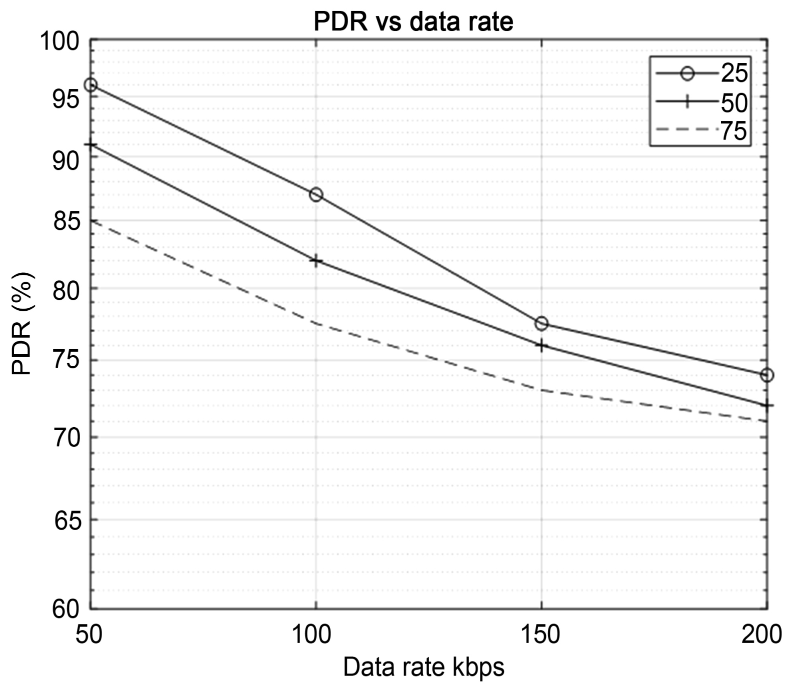

Figure 3. PDR versus data rate for different network node density in the presence of strong t turbulence.

the same date rate. For instance, at 150 kbps and in the presence of strong turbulence with 25, 50, and 75 nodes, the PDRs are 77%, 76%, and 73% respectively. Further, at 150 kbps and with a number of nodes of 75 nodes, the achieved throughput is 2100 kbps only.

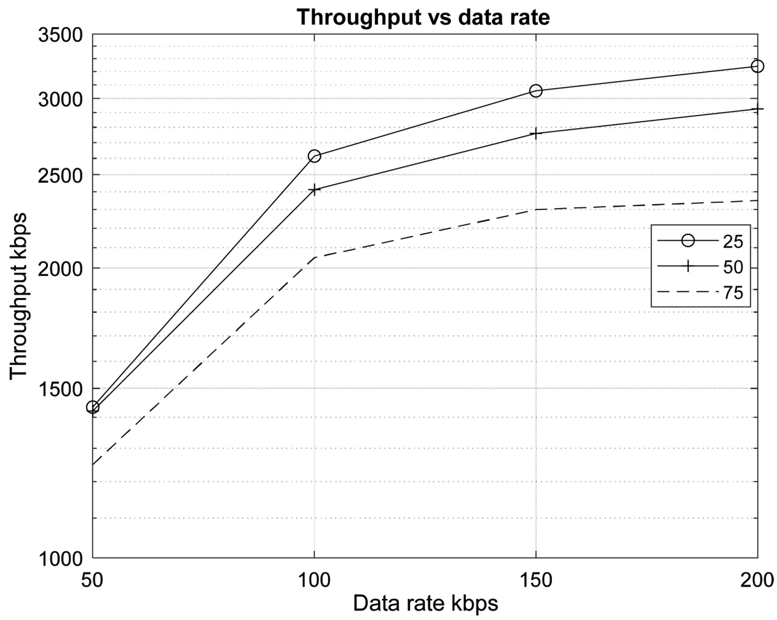

Figure 4. Throughput versus data rate for different network node density in the presence of weak turbulence.

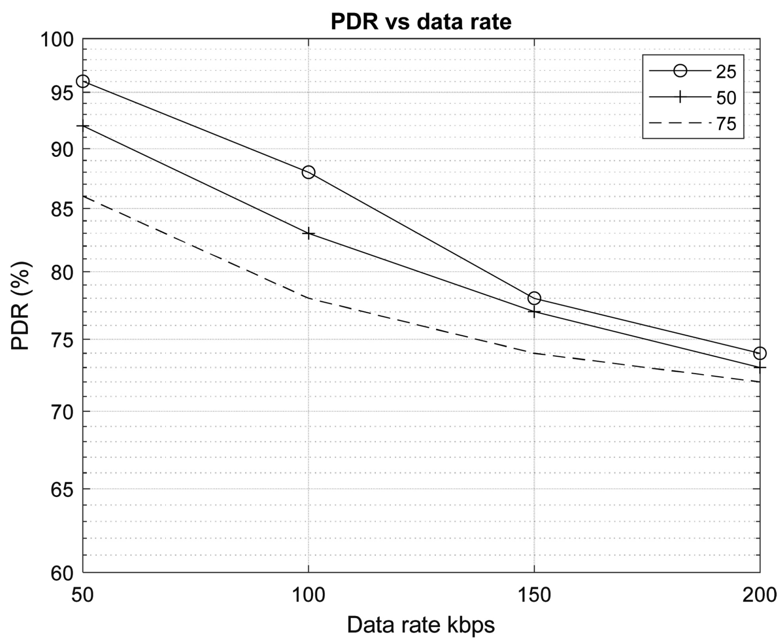

Figure 5. PDR versus data rate for different network node density in the presence of weak turbulence.

Further, in order to have a more comprehensive study of FSO on MANETs with the presence of atmospheric turbulence, the impact of mobility, especially the mobility speed will be investigated in our future research work.

Conflicts of Interest

The authors declare no conflicts of interest regarding the publication of this paper.

References

[1] Shafi, M., Molisch, A.F., Smith, P.J., Haustein, T., Zhu, T., De Silva, P., Tufvesson, F., Benjebbour, A. and Wunder, G. (2017) 5G: A Tutorial Overview of Standards, Trials, Challenges, Deployment, and Practice. *IEEE Journal on Selected Areas in Communications*, **35**, 1201-1221. https://doi.org/10.1109/JSAC.2017.2692307

[2] Nokia Networks (2014) 5G Use Cases and Requirements. https://www.ramonmillan.com/documentos/bibliografia/5GUseCases_Nokia.pdf

[3] Arnon, S., Barry, J., Karagiannidis, G., Schober, R. and Uysal, M. (2012) Advanced Optical Wireless Communication Systems. Cambridge University Press, Cambridge. https://doi.org/10.1017/CBO9780511979187

[4] Akella, J., Yuksel, M. and Kalyanaraman, S. (2005) Error Analysis of Multi-Hop Free-Space-Optical Communication. *Proceedings of IEEE International Conference on Communications*, 2005 (*ICC* 2005), Seoul, 16-20 May 2005, 1777-1781.

[5] Akella, J., Yuksel, M., Kalyanaraman, S. and Dutta, P. (2009) Free-Space-Optical Mobile ad hoc Networks: Auto-Configurable Building Blocks. *Wireless Networks*, **15**, 295-312. https://doi.org/10.1007/s11276-007-0040-y

[6] Nakhkoob, B., Bilgi, M., Yuksel, M. and Hella, M. (2009) Multi-Transceiver Optical Wireless Spherical Structures for MANETs. *IEEE Journal on Selected Areas of Communications*, **27**, 1612-1622. https://doi.org/10.1109/JSAC.2009.091211

[7] George, D. and Sankar, S.P. (2016) Stability Routing in FSO-MANET. *International Journal of Research in Engineering and Technology*, **5**, 216-220.

[8] Devi, S. and Sarje, A. (2015) Dir-DREAM: Geographical Routing Protocol for FSO MANET. In: Buyya, R. and Thampi, S., Eds., *Intelligent Distributed Computing. Advances in Intelligent Systems and Computing*, Vol. 321, Springer, Cham, 95-106. https://doi.org/10.1007/978-3-319-11227-5_9

[9] Recolons, J., Andrews, L.C. and Phillips, R.L. (2007) Analysis of Beam Wander Effects for a Horizontal-Path Propagating Gaussian-Beam Wave: Focused Beam Case. *Optical Engineering*, **46**, Article ID: 086002. https://doi.org/10.1117/1.2772263

[10] Barrios, R. and Dios, F. (2012) Exponentiated Weibull Distribution Family under Aperture Averaging for Gaussian Beam Waves. *Optics Express*, **20**, 13055-13064. https://doi.org/10.1364/OE.20.013055

[11] Andrews, L.C. (1992) Aperture-Averaging Factor for Optical Scintillations of Plane and Spherical Waves in the Atmosphere. *Journal of the Optical Society of America A*, **9**, 597-600. https://doi.org/10.1364/JOSAA.9.000597

[12] Ali, M.A. (2014) Comparison of NRZ, RZ-OOK Modulation Formats for FSO Communications under Fog Weather Condition. *International Journal of Computer Applications*, **108**, 29-34.

[13] Majumdar, A.K. (2015) Advanced Free Space Optics (FSO): A System Approach. Vol. 186, 1st Edition, Springer, New York.

[14] Majumdar, A.K. and Ricklin, J.C. (2008) Free-Space Laser Communications: Principles and Advances. Springer, New York. https://doi.org/10.1007/978-0-387-28677-8

[15] Yi, X., Liu, Z.J. and Yue, P. (2012) Average BER of Free-Space Optical Systems in Turbulent Atmosphere with Exponentiated Weibull Distribution. *Optics Letters*, **37**, 5142-5144. https://doi.org/10.1364/OL.37.005142

[16] Barrios, R. and Dios, F. (2012) Probability of Fade and BER Performance of FSO Links over the Exponentiated Weibull Fading Channel under Aperture Averaging.

Proceedings SPIE Conference Unmanned/ *Unattended Sensors and Sensor Networks IX*, **8540**, Article ID: 85400D. https://doi.org/10.1117/12.974646

[17] Senior, J.M. and Jamro, M.Y. (2009) Optical Fiber Communications: Principles and practice. 3rd Edition, Pearson Education Ltd., London.

[18] Kumar, P. (2015) Comparative Analysis of BER Performance for Direct Detection and Coherent Detection FSO Communication Systems. 5*th International Conference on Communication Systems and Network Technologies*, Gwalior, 4-6 April 2015, 369-374. https://doi.org/10.1109/CSNT.2015.42

[19] Press, W.H., Teukolsky, S.A., Vetterling, W.A. and Flannery, B.P. (1992) Numerical Recipies in C: The Art of Scientific Computing. Cambridge University Press, Cambridge.

[20] Jevtic, N. and Malnar, M. (2019) Novel ETX-Based Metrics for Overhead Reduction in Dynamic Ad Hoc Networks. *IEEE Access*, **7**, 116490-116504. https://doi.org/10.1109/ACCESS.2019.2936191